Superlattices and Microstructures 140 (2020) 106435

Contents lists available at ScienceDirect

Superlattices and Microstructures

journal homepage: www.elsevier.com/locate/yspmi

Modulation of electronic and optical properties of GaTe monolayer by biaxial strain and electric field

Vo T.T. Vi [a], Nguyen N. Hieu [b], Bui D. Hoi [a], Nguyen T.T. Binh [b], Tuan V. Vu [c,d,*]

[a] Department of Physics, University of Education, Hue University, Hue, Viet Nam
[b] Institute of Research and Development, Duy Tan University, Da Nang, Viet Nam
[c] Division of Computational Physics, Institute for Computational Science, Ton Duc Thang University, Ho Chi Minh City, Viet Nam
[d] Faculty of Electrical & Electronics Engineering, Ton Duc Thang University, Ho Chi Minh City, Viet Nam

ARTICLE INFO

Keywords:
Monolayer GaTe
Electronic and optical properties
Strain engineering
External electric field
Density functional theory

ABSTRACT

In this work, the electronic and optical properties of monolayer GaTe under biaxial strain and external electric field were investigated by density functional theory. Our calculated results indicate that the monolayer GaTe is an indirect-semiconductor with an energy gap of 1.41 eV at equilibrium. Electronic properties of monolayer GaTe, especially the energy gap, depend greatly on the biaxial strain and external electric field. While the compressive strain slightly increases the energy gap, the tensile strain reduces quite rapidly the energy gap of the monolayer GaTe. In particular, semiconductor–metal phase transition can be observed when the external electric field was introduced. The GaTe monolayer strongly absorbs light in the ultraviolet region and the biaxial strain greatly changes its optical characteristics, especially the compression strain significantly increasing the absorption coefficient of the monolayer. Our results can provide more useful information for the prospect of application of the GaTe monolayer in next-generation optoelectronic devices.

1. Introduction

Since its discovery in 2004 [1], graphene has become one of the most attractive nanomaterials due to its extraordinary chemical and physical properties which have a lot of promising applications in nanotechnology. Graphene has made a huge breakthrough in nanotechnology devices with many amazing applications [2–6]. However, with its semi-metallic form, graphene has encountered many difficulties in its application in optoelectronic devices, such as field-effect transistors [7]. In parallel with finding a way to overcome the disadvantages of graphene, a large-scale search for two-dimensional (2D) graphene-like materials [8–10] took place and obtained many excellent results [11–15]. Silicene, germanene, phosphorene, dichalcogenides, and monochalcogenides have been successfully synthesized experimentally. The family of layered 2D materials is increasingly expanding and with many potential applications in next-generation devices [16–22].

Gallium telluride (GaTe) a typical material of group III monochalcogenides with many physical properties that differ from other materials in this group [23]. Recently GaTe nanosheet has been synthesized successfully by the common experimental method of chemical vapor deposition [24]. Through analysis of phonon dispersion curves, Demirci et al. showed that GaTe monolayer is dynamically stable and monolayer GaTe is a semiconductor with an indirect bandgap of 1.43 eV using the Perdew, Burke, and Ernzerhof (PBE) method [23]. The problem of the energy gap of semiconductors can be accurately estimated with the hybrid functional. However, the band structures calculated with these functionals have the same profile. Ren and co-workers showed

* Corresponding author at: Division of Computational Physics, Institute for Computational Science, Ton Duc Thang University, Ho Chi Minh City, Viet Nam.
E-mail addresses: hieunn@duytan.edu.vn (N.N. Hieu), vuvantuan@tdtu.edu.vn (T.V. Vu).

https://doi.org/10.1016/j.spmi.2020.106435
Received 21 December 2019; Received in revised form 15 January 2020; Accepted 10 February 2020
Available online 13 February 2020

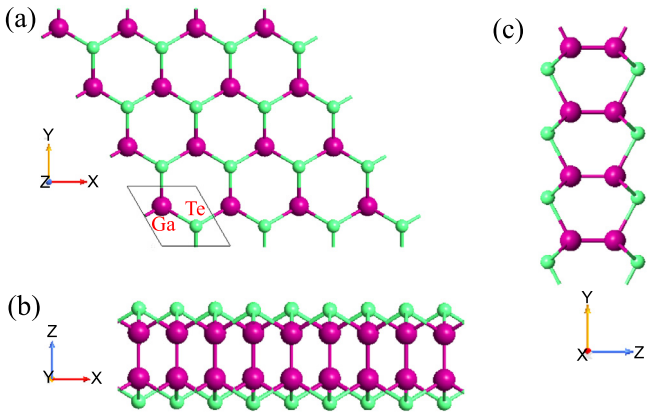

Fig. 1. Top (a), side (b) and front (c) views of atomic structure of GaTe monolayer.

that GaTe monolayer possesses catalytic properties and can be applied as photocatalyst for water splitting [25]. Recently, the influence of strain on the mechanical properties and electronic states of the GaTe monolayer has been studied through first-principles calculations [26]. It has been shown that the bandgap of the GaTe monolayer depends greatly on strain engineering, particularly in the tensile case [26]. Besides, modulation of the electronic properties of the GaTe monolayer by its surface functionalization has also been investigated recently [27]. Also, the ability to apply monolayer GaTe to optoelectronic devices and gas sensors has been studied [28–30]. Previous studies have shown that the band gap of the group III monochalcogenide monolayers, such as monolayers InSe and GaS, is reduced when the electric field is introduced [31–34]. In particular, based on the analyzes of the charge polarization and its influence on the structural properties, Wang et al. showed that the charge polarization of InSe monolayer depends strongly on intensity and direction of external electric field [33] and the change of charge polarization due to electric field can lead to slightly change in geometrical structure of monolayer. The In–Se bond length has different values when the electric field has different directions. As a result, the band structure of InSe monolayer under electric field is not the same in cases of negative and positive electric fields (with different directions). In parallel to supporting studies for monolayers [32,34], van der Waals heterostructure based on two-dimensional (2D) group III monochalcogenides have been studied seriously in recently [35–39].

In the present study, we investigate the electronic and optical properties of the GaTe monolayer under an external electric field E and biaxial strain ε_b by density functional theory. The influence of the E and ε_b on the band structure and energy gap of monolayer GaTe has been carefully investigated. Besides, based on the achieved results, the possibility of application of monolayer GaTe into nanoelectronic devices has been discussed.

2. Computational detail

In this work, we investigate the structural parameters and electronic states of monolayer GaTe by density functional theory (DFT) via the Quantum ESPRESSO package [40] with the generalized gradient approximations (GGA). We used the accurate projector augmented-wave method [41,42] and the PBE functional [43,44] in our studies. To estimate the weak van der Waals interactions in the 2D material, we used also the DFT-D2 semi-empirical method [45]. For sampling the first Brillouin zone, the $(15 \times 15 \times 1)$ k-mesh grid was used in this work. A supercell of (4×4) for monolayer GaTe was built for the simulations. The cut-off of energy for the plane-wave basis was set as 37 Ry. In this work, all structures of monolayers are fully optimized with convergence criteria for the force acting on each atom less than 10^{-6} Ry/cell. A 20 Å vacuum space along the z-axis is adopted to eliminate the interactions between neighbor layers. All calculations for structural parameters, both strained and unstrained cases, were optimized to get the atomic positions at equilibrium in its unit-cell.

3. Results and discussion

The GaTe is one of the typical compounds of group III–VI monochalcogenides which is formed from four atomic layers stacking in the Te–Ga–Ga–Te order as shown in Fig. 1. In its honeycomb form, there are 4 atoms in a unit cell (two Te and two Ga atoms) and GaTe belongs to the D_{3h} group symmetry. The constant lattice of the monolayer GaTe at equilibrium is $a = 4.08$ Å. The Ga–Ga and Ga–Te bond lengths are respectively $d_{\text{Ga–Ga}} = 2.68$ Å and $d_{\text{Ga–Te}} = 2.45$ Å. The monolayer thickness (distance between the top and bottom Te layers) is $h = 5.00$ Å. Our findings are consistent with the previous theoretical studies [23,46].

Monolayer GaTe is an indirect semiconductor at equilibrium and its bandgap is 1.41 eV as depicted in Fig. 2. Our calculated result is in good agreement with the available data from previous DFT studies [23,27,28]. This bandgap of the monolayer GaTe is in the energy region of the visible light which can make the monolayer GaTe being a potential candidate for applications in photodetectors. Also, the necessary condition for a material to possess photocatalytic activities is that its minimum bandgap must be larger than 1.23 eV because of the standard oxidation potential of the O_2/H_2O at the $pH = 0$ being 1.23 eV vs. the normal

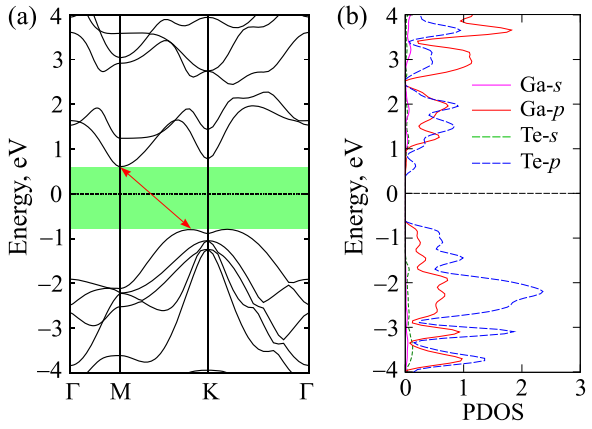

Fig. 2. (a) Band structure and (b) PDOS of the GaTe monolayer at equilibrium.

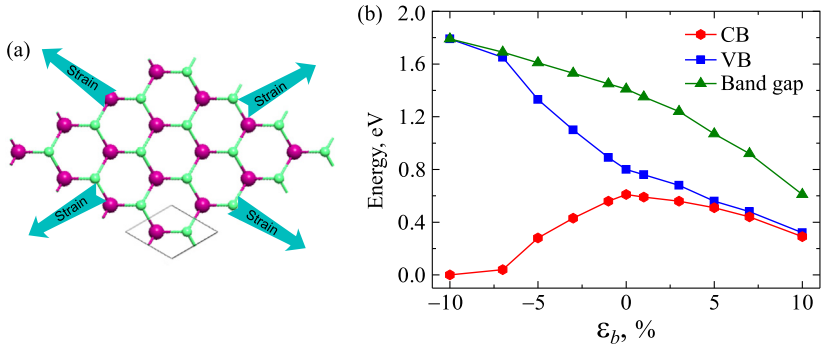

Fig. 3. (a) Model of monolayer GaTe under a biaxial strain and (b) dependence of the lowest energy of the conduction band (CB), the highest energy of the valence band (VB) and bandgap of GaTe monolayer on the ε_b.

hydrogen electrode. Therefore, with the bandgap of 1.41 eV, the monolayer GaTe can be possessed photocatalytic activities for water splitting applications. Previous study has demonstrated that the GGA-PBE functional underestimates the energy gap of the semiconductor materials [47]. It is well-known that the problem of calculating energy gap accurately can be solved using the Heyd–Scuseria–Ernzerhof (HSE06) hybrid functional [48] or GW method [49]. However, the calculated electronic structure of monolayer using the GGA-PBE and HSE06 functionals are the same profile. The fundamental characteristics of the electronic structure of the layered monolayers are unchanged whether they are estimated by GGA-PBE or HSE06 functionals. We can see that the conduction band minimum locates at the M-point and the valence band maximum is on the MK-path. Focusing on the valence band maximum, we find that, the valence band maximum locates very close to the K-point and energy difference between the valence band maximum and the maximum point of the valence band at the K-point is quite small. Besides, we can also expect a change of the position the conduction band minimum from the M-point to the K-point when the external conditions, such as external electric field, applied pressure or strain engineering, are applied. These changes may cause the transition from indirect to direct bandgap in the GaTe monolayer. To see the contribution of orbitals of the Ga and Te atoms to the electronic bands of the monolayer GaTe, we calculate the partial density of states (PDOS) of the monolayer GaTe as shown in Fig. 2(b). Our calculations have shown that while the electronic bands of the monolayer GaTe are mainly contributed from the Ga-*p* and Te-*p* orbital, the contribution of the Ga-*s* and Te-*s* orbitals to the formation of the electronic band is negligible. From Fig. 2(b) we can see that the contribution of the Ga-*p* orbitals to the conduction band is predominant, while the contribution of the Te-*p* orbitals to the valence band is greater than that of the Ga-*p* orbitals.

We next consider the electronic properties of the GaTe monolayer when a strain engineering was introduced. The schematic model of monolayer GaTe under biaxial strain is illustrated in Fig. 3(a). To quantitatively estimate the effect of strain on the electronic properties of a monolayer GaTe, we define the biaxial strain as $\varepsilon_b = (\Lambda - \Lambda_0)/\Lambda_0$, where Λ_0 and Λ are respectively stand for the lattice constants of a monolayer GaTe before and after strain. In this study, a large range of the biaxial strain ε_b from −10% to 10% is applied to the GaTe monolayer. A negative value of the ε_b is implied as compressive biaxial strain and positive one refers to the tensile strain. It is well-known that the group III-monochalcogenides have excellent mechanical properties. Previous theoretical studies have been demonstrated that the critical uniaxial strain along the armchair (zigzag) direction of the III-monochalcogenide InSe monolayer is up to 27% (25%) [50]. Also, from calculations for the strain–stress relations and Young's modulus, one indicated

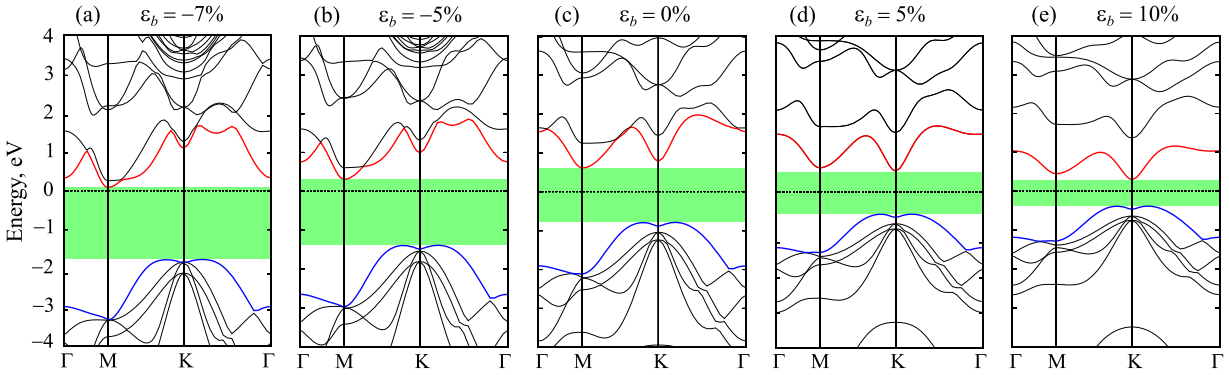

Fig. 4. (a) Band structure of GaTe monolayer under different values of strain ε_b.

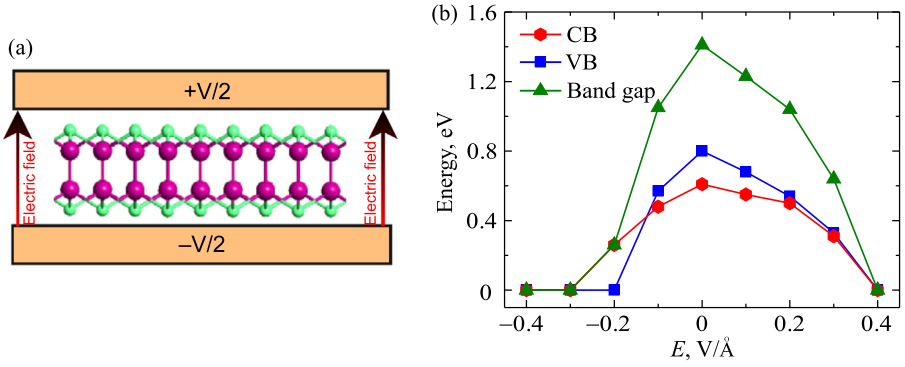

Fig. 5. Model of monolayer GaTe under an electric field (a) and dependence of the CB, VB and band gap on electric field E.

that the critical strain limit is close to that found in other 2D layered materials such as phosphorene which is stable under applied strain from 16% to 20% [51]. Therefore, we believe that the structure of a monolayer GaTe will be stable under the small biaxial strain from −10% to 10%. Our DFT calculations demonstrated that while compressive strain $\varepsilon_b < 0$ increases the bandgap E_g of the monolayer GaTe, the E_g of the GaTe monolayer is greatly reduced in the presence of tensile biaxial strain. Dependence of the bandgap of the monolayer GaTe on the biaxial strain is illustrated in Fig. 3(b). As shown in Fig. 3(b), the bandgap of the monolayer is linearly dependent on individually the compressive and tensile biaxial strains. However, tensile strain tends to reduce the energy gap of the monolayer GaTe faster than the increase of the E_g due to compressive strain. In Fig. 3(b) we show also the lowest energy of the conduction band (CB) and the highest energy of the valence band (VB). We can see that the tensile strain causes both the CB and VB to be closer to the Fermi level $E_F = 0$ and they are almost symmetrical to each other through the Fermi level at large elongations. Its consequence is the reduced bandgap of monolayer GaTe as the above-mentioned. However, in contrast to the case of tensile strain, the compressive strain causes an abnormal change in the CB and VB. Under the influence of compression biaxial strain, while the CB tends to move closer to the Fermi level, the VB has pushed away from the Fermi level. Besides, strain engineering not only changes the value of the CB and VB but also can change the position of the conduction band minimum and the valence band maximum. Our obtained results indicate that the strain engineering has significantly modulated the electronic energy band structure, particularly the conduction band, of the GaTe monolayer. Influence of the ε_b on the band structure of GaTe monolayer is illustrated in Fig. 4. As shown in Fig. 4, the position of the conduction band minimum is moved from the M- to the K-point due to the tensile biaxial strain. Compressive strain makes the CM closer to the Fermi level but does not change the position of the conduction band minimum.

So far, the group III monochalcogenides have been extensively studied recently. However, these studies mainly focused on the group III monochalcogenides containing chalcogen atoms of S and Se [33,52]. The absence of studies of the group III monochalcogenides containing the Te atoms such as GaTe or InTe has left a fairly large gap, especially these materials in the electric field E. In this part, we examine the influence of an external electric field on the electronic properties of the monolayer GaTe. The model of monolayer GaTe in a perpendicular E is depicted in Fig. 5(a). As illustrated in Fig. 5(a), the external electric field is perpendicular to the 2D surface of the material. The direction of the **E** is along with the z-axis. The $E < 0$ implies that the **E** and the z-axis are the opposite. In the present study, we investigate the electronic structure of the monolayer under the electric field with the magnitude varying from −0.4 V/Å to 0.4 V/Å. Our DFT estimations indicate that the bandgap of the GaTe monolayer GaTe depends greatly on the electric field E. We can see that the electronic structure of the monolayer is significantly changed due to the electric field, especially the conduction band. The consequence of this change is a drastic change in the energy gap when

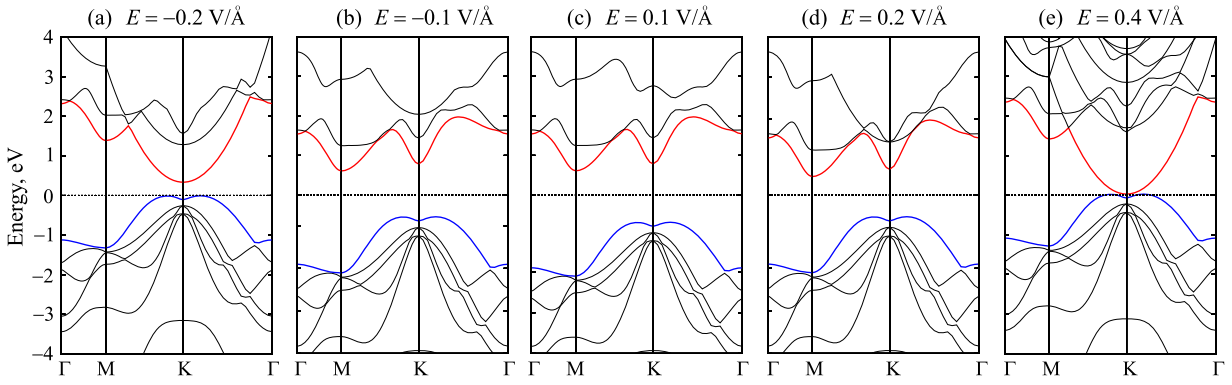

Fig. 6. (a) Band structure of GaTe monolayer under electric field E.

the electric field is applied. We see that the electric field significantly reduces the bandgap of a monolayer GaTe as illustrated in Fig. 5(b). Besides, the electric field is responsible for the decrease in the bandgap of the monolayer GaTe, in both positive and negative electric fields. In particular, the bandgap of the monolayer GaTe decreases to zero when the external electric field is equal to 0.4 V/Å. We can conclude that the phase transition from semiconductor to metal has been observed in the GaTe monolayer at the large electric field of $E = 0.4$ V/Å.

Fig. 6 indicates that the band structures of the GaTe monolayer are different in the cases of negative and positive fields. It is well-known that the charge polarization in the monolayer depends on the directions of the **E** and the change in charge polarization due to the applied electric field can lead to geometrical changes [33]. This is the cause of the difference in band structures of the GaTe monolayer in the cases of negative/positive fields as shown in Fig. 6.

Band structure of monolayer GaTe under different values of the E is shown in Fig. 6. Unlike GaS or GaSe monolayers, the influence of the E on the band structure of the GaTe monolayer is significant, especially in the high electric field region. While the valence band only shifted closer to the Fermi level due to the applied electric field, the conduction band is strongly influenced by the external electric field. The electric field not only changes the position of the conduction band minimum but also causes semiconductor–metal phase transition in the monolayer GaTe as above-mentioned. As clearly shown in Fig. 6, the external electric field tends to shift the position of the conduction band minimum from the M- to the K-point. The conduction band minimum has moved to the K-point when the external electric field is large enough. Controlling the electronic properties of the monolayer GaTe by electric field or strain engineering, especially the phase transition from semiconductor to metal due to effects of the electric field, can make the GaTe monolayer becoming a potential candidate for applications in next-generation nanoelectronic devices.

In the next part, we present our calculations for the basic optical characteristics of the GaTe monolayer under the ε_b and electric field E. The dielectric function $\varepsilon(\omega)$ can be defined as

$$\varepsilon(\omega) = \varepsilon_1(\omega) + i\varepsilon_2(\omega), \tag{1}$$

where $\varepsilon_1(\omega)$ and $\varepsilon_2(\omega)$ are respectively the real and imaginary parts of the $\varepsilon(\omega)$. We first can obtain the $\varepsilon_2(\omega)$ via sum of the occupied–unoccupied transitions and the real part $\varepsilon(\omega)$ can be then received via the Kramer–Kronig transformation [53,54]:

$$\varepsilon_2^{ij}(\omega) = \frac{Ve^2}{2\pi\hbar m^2\omega^2}\int d^3\mathbf{k}\sum_{nn'}\langle \mathbf{k}n\left|p_i\right|\mathbf{k}n'\rangle\langle \mathbf{k}n'\left|p_j\right|\mathbf{k}n\rangle \times f_{\mathbf{k}n}(1-f_{\mathbf{k}n'})\delta(E_{\mathbf{k}n'}-E_{\mathbf{k}n}-\hbar\omega) \tag{2}$$

and

$$\varepsilon_1(\omega) = 1 + \frac{2}{\pi}P\int_0^\infty \frac{\omega'\varepsilon_2(\omega')}{\omega'^2-\omega^2}d\omega', \tag{3}$$

where ω is the angular frequency, e/m is the electron charge/mass, V is the unit cell volume, $p = (p_x, p_y, p_z)$ is the momentum operator, $|knp\rangle$ is the wave function with the wavevector **k**, and f_{kn} is the Fermi distribution function.

The absorption coefficient $A(\omega)$ is written as follows [55]

$$A^{ij}(\omega) = \frac{\omega\sqrt{2}}{c}\left[\sqrt{\varepsilon_1^{ij}(\omega)^2+\varepsilon_2^{ij}(\omega)^2}-\varepsilon_1^{ij}(\omega)\right]^{1/2}. \tag{4}$$

In Fig. 7, we present the calculated results for the real and imaginary parts of the dielectric function of the GaTe monolayer in the presence of the ε_b and E. At equilibrium, the first optical gap is at 3.780 eV as shown in Fig. 7. From Fig. 7, we can see that while the influence of the E on the dielectric function is negligible, both $\varepsilon_1(\omega)$ and $\varepsilon_2(\omega)$ depend greatly on the ε_b, particularly in the range from 0 to 7 eV of incident light energy. When the ε_b was introduced, the first optical gap has shifted significantly. Under the compressive strain $\varepsilon_b < 0$, the first optical gap shifts to a higher energy domain while it will shift to a lower energy

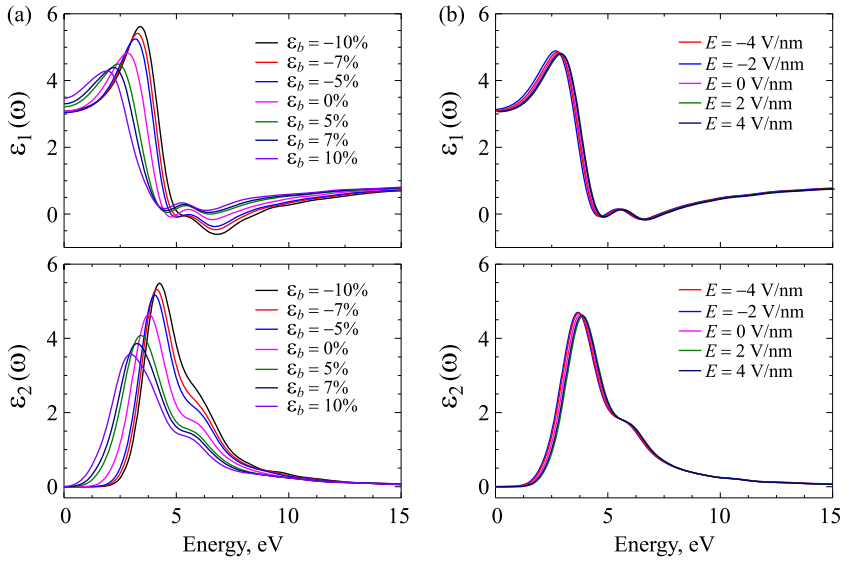

Fig. 7. The $\varepsilon_1(\omega)$ and $\varepsilon_2(\omega)$ of the GaTe monolayer under (a) strain ε_b and (b) electric field.

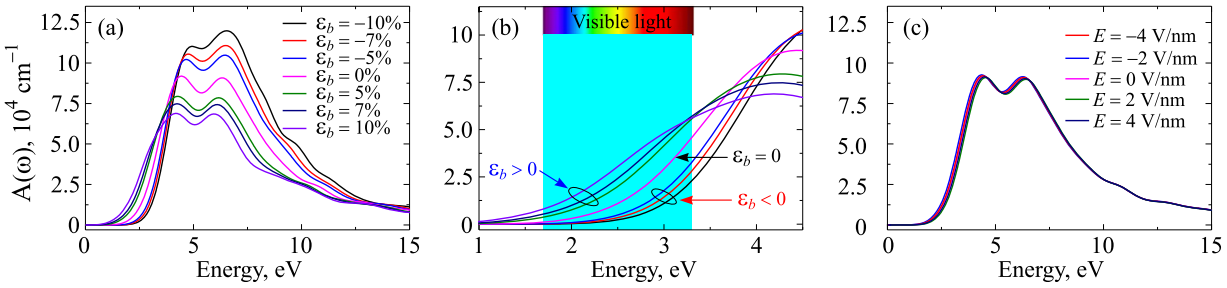

Fig. 8. Absorption coefficient $A(\omega)$ of GaTe monolayer under strain ε_b (a,b) and electric field (c). Figure (b) is the enlargement of figure (a) in the visible light region.

domain if affected by the tensile biaxial strain. Previous DFT calculations also indicated that the effect of the E on the basic optical characteristics of 2D layered materials, such as Janus ZrSSe monolayer [56], is negligible.

The influence of the ε_b and E on the absorption coefficient $A(\omega)$ of the GaTe monolayer is depicted in Fig. 8. At equilibrium, the maximum of absorption coefficient $A(\omega)_{\max}$ is 9.189×10^4 cm^{-1} at the photon energy of 4.445 eV. Focusing on the case of the GaTe monolayer under biaxial strain as illustrated in Fig. 8(a), we can see that tensile strain reduces the $A(\omega)_{\max}$ while the $A(\omega)_{\max}$ increases under the compressive strain. Compressive strain increases the $A(\omega)_{\max}$ up to 11.983×10^4 cm^{-1} at $\varepsilon_b = -10\%$. The calculated results demonstrated that the GaTe monolayer absorbs strongly light in the ultraviolet region. In the visible light region, the effect of the ε_b on the $A(\omega)$ is very interesting. Contrary to the changing trend of the $A(\omega)_{\max}$ due to the strain as above-analyzed, the $A(\omega)$ of the GaTe monolayer is reduced in the presence of compressive strain while the tensile strain increases significantly $A(\omega)$ as depicted in Fig. 8(b). Fig. 8(c) shows the absorption coefficient in the presence of an electric field. The dependence of the $A(\omega)$ on the E in the GaTe monolayer is negligible.

4. Conclusion

In conclusion, the structural and electronic properties of monolayer GaTe under biaxial strain and external electric field are systematically investigated using DFT calculations. Our DFT calculations demonstrated that the GaTe monolayer is an indirect-semiconductor and we can modulate it by strain or external electric field. We have also shown that electric fields can lead to the transition from semiconductor to metal in the GaTe monolayer, which can be very useful in applications for nanoelectromechanical devices. While the influence of the electric field on the optical characteristics is negligible, biaxial strain significantly shifts the optical peaks and greatly alters the absorption coefficient in the GaTe monolayer. Our results may give helpful information for the applicability of the GaTe monolayer into next-generation optoelectronic devices.

Declaration of competing interest

The authors declare that they have no known competing financial interests or personal relationships that could have appeared to influence the work reported in this paper.

CRediT authorship contribution statement

Vo T.T. Vi: Software, Conceptualization, Methodology, Investigation, Validation, Funding acquisition, Writing - original draft. **Nguyen N. Hieu:** Conceptualization, Supervision, Writing - original draft, Writing - review & editing. **Bui D. Hoi:** Conceptualization, Software, Investigation, Validation, Writing - original draft. **Nguyen T.T. Binh:** Validation, Writing - review & editing. **Tuan V. Vu:** Methodology, Software, Investigation, Writing - review & editing.

Acknowledgments

This work was supported by the Domestic Master/PhD Scholarship Programme of Vingroup Innovation Foundation.

References

[1] K.S. Novoselov, A.K. Geim, S.V. Morozov, D. Jiang, Y. Zhang, S.V. Dubonos, I.V. Grigorieva, A.A. Firsov, Science 306 (2004) 666.
[2] V. Skrypnychuk, N. Boulanger, V. Yu, M. Hilke, S.C.B. Mannsfeld, M.F. Toney, D.R. Barbero, Adv. Funct. Mater. 25 (2015) 664.
[3] M. Yarmohammadi, AIP Adv. 6 (2016) 085008.
[4] H. Wang, D. Nezich, J. Kong, T. Palacios, IEEE Electron Device Lett. 30 (2009) 547.
[5] M. Yarmohammadi, M. Zareyan, Chin. Phys. B 25 (2016) 068105.
[6] J. Wu, M. Agrawal, H.A. Becerril, Z. Bao, Z. Liu, Y. Chen, P. Peumans, ACS Nano 4 (2010) 43.
[7] F. Schwierz, Nat. Nanotechnol. 5 (2010) 487.
[8] M. Yarmohammadi, Solid State Commun. 253 (2017) 57.
[9] P.T.T. Le, M. Davoudiniya, M. Yarmohammadi, Phys. Chem. Chem. Phys. 21 (2019) 238.
[10] M. Yarmohammadi, RSC Adv. 7 (2017) 10650.
[11] M. Yarmohammadi, Phys. Lett. A 381 (2017) 1261.
[12] M.M. Obeid, H.R. Jappor, K. Al-Marzoki, D. Hoat, T.V. Vu, S.J. Edrees, Z.M. Yaseen, M.M. Shukur, Comput. Mater. Sci. 170 (2019) 109201.
[13] M. Yarmohammadi, J. Magn. Magn. Mater. 426 (2017) 621.
[14] H.D. Bui, H.R. Jappor, N.N. Hieu, Superlattices Microstruct. 125 (2019) 1.
[15] M. Yarmohammadi, J. Electron. Mater. 45 (2016) 4958.
[16] A.A. Attia, H.R. Jappor, Chem. Phys. Lett. 728 (2019) 124.
[17] H. Bui, M. Yarmohammadi, Solid State Commun. 280 (2018) 39.
[18] H.R. Jappor, M.A. Habeeb, Curr. Appl. Phys. 18 (2018) 673.
[19] P. Le, M. Yarmohammadi, Physica E 107 (2019) 11.
[20] A.O.M. Almayyali, B.B. Kadhim, H.R. Jappor, Physica E 118 (2020) 113866.
[21] M. Yarmohammadi, Solid State Commun. 250 (2017) 84.
[22] H.T. Nguyen, T.V. Vu, N.T. Binh, D. Hoat, N.V. Hieu, N.T. Anh, C.V. Nguyen, H.V. Phuc, H.R. Jappor, M.M. Obeid, N.N. Hieu, Chem. Phys. 529 (2020) 110543.
[23] S. Demirci, N. Avazli, E. Durgun, S. Cahangirov, Phys. Rev. B 95 (2017) 115409.
[24] Z. Wang, M. Safdar, M. Mirza, K. Xu, Q. Wang, Y. Huang, F. Wang, X. Zhan, J. He, Nanoscale 7 (2015) 7252.
[25] C. Ren, S. Wang, H. Tian, Y. Luo, J. Yu, Y. Xu, M. Sun, Sci. Rep. 9 (2019) 13289.
[26] L. Huang, Z. Chen, J. Li, RSC Adv. 5 (2015) 5788.
[27] S. Zhou, C.-C. Liu, J. Zhao, Y. Yao, NPJ Quantum Mater. 3 (2018) 16.
[28] S.S. Abed Al-Abbas, M.K. Muhsin, H.R. Jappor, Chem. Phys. Lett. 713 (2018) 46.
[29] S. Huang, Y. Tatsumi, X. Ling, H. Guo, Z. Wang, G. Watson, A.A. Puretzky, D.B. Geohegan, J. Kong, J. Li, T. Yang, R. Saito, M.S. Dresselhaus, ACS Nano 10 (2016) 8964.
[30] S.S. Abed Al-Abbas, M.K. Muhsin, H.R. Jappor, Superlattices Microstruct. 135 (2019) 106245.
[31] F. Guo, Y. Wu, Z. Wu, C. Ke, C. Zhou, T. Chen, H. Li, C. Zhang, M. Fu, J. Kang, Nanoscale Res. Lett. 12 (2017) 409.
[32] D.Q. Khoa, D.T. Nguyen, C.V. Nguyen, V.T. Vi, H.V. Phuc, L.T. Phuong, B.D. Hoi, N.N. Hieu, Chem. Phys. 516 (2019) 213.
[33] X.-P. Wang, X.-B. Li, N.-K. Chen, J.-H. Zhao, Q.-D. Chen, H.-B. Sun, Phys. Chem. Chem. Phys. 20 (2018) 6945.
[34] K.D. Pham, V.T. Vi, D.V. Thuan, N.V. Hieu, C.V. Nguyen, H.V. Phuc, B.D. Hoi, L.T. Phuong, N.Q. Cuong, D.V. Lu, N.N. Hieu, Chem. Phys. 524 (2019) 101.
[35] P.T.T. Le, N.N. Hieu, L.M. Bui, H.V. Phuc, B.D. Hoi, B. Amin, C.V. Nguyen, Phys. Chem. Chem. Phys. 20 (2018) 27856.
[36] K.D. Pham, L.G. Bach, B. Amin, M. Idrees, N.N. Hieu, H.V. Phuc, H.D. Bui, C.V. Nguyen, J. Appl. Phys. 125 (2019) 225304.
[37] H.V. Phuc, N.N. Hieu, B.D. Hoi, C.V. Nguyen, Phys. Chem. Chem. Phys. 20 (2018) 17899.
[38] K.D. Pham, C.V. Nguyen, H.T. Phung, H.V. Phuc, B. Amin, N.N. Hieu, Chem. Phys. 521 (2019) 92.
[39] H.V. Phuc, V.V. Ilyasov, N.N. Hieu, B. Amin, C.V. Nguyen, J. Alloys Compd. 750 (2018) 765.
[40] P. Giannozzi, S. Baroni, N. Bonini, M. Calandra, R. Car, C. Cavazzoni, D. Ceresoli, G.L. Chiarotti, M. Cococcioni, I. Dabo, A.D. Corso, S. de Gironcoli, S. Fabris, G. Fratesi, R. Gebauer, U. Gerstmann, C. Gougoussis, A. Kokalj, M. Lazzeri, L. Martin-Samos, N. Marzari, F. Mauri, R. Mazzarello, S. Paolini, A. Pasquarello, L. Paulatto, C. Sbraccia, S. Scandolo, G. Sclauzero, A.P. Seitsonen, A. Smogunov, P. Umari, R.M. Wentzcovitch, J. Phys.: Condens. Matter 21 (2009) 395502.
[41] P.E. Blöchl, Phys. Rev. B 50 (1994) 17953.
[42] G. Kresse, D. Joubert, Phys. Rev. B 59 (1999) 1758.
[43] J.P. Perdew, K. Burke, M. Ernzerhof, Phys. Rev. Lett. 77 (1996) 3865.
[44] J.P. Perdew, K. Burke, M. Ernzerhof, Phys. Rev. Lett. 78 (1997) 1396.
[45] S. Grimme, J. Comput. Chem. 27 (2006) 1787.
[46] A.V. Kosobutsky, S.Y. Sarkisov, Phys. Solid State 60 (2018) 1686.
[47] J.P. Perdew, M. Levy, Phys. Rev. Lett. 51 (1983) 1884.

[48] J. Heyd, G.E. Scuseria, M. Ernzerhof, J. Chem. Phys. 118 (2003) 8207.
[49] L. Hedin, Phys. Rev. 139 (1965) A796.
[50] T. Hu, J. Zhou, J. Dong, Phys. Chem. Chem. Phys. 19 (2017) 21722.
[51] T. Hu, J. Dong, Phys. Rev. B 92 (2015) 064114.
[52] S.-D. Guo, Y.-H. Wang, J. Appl. Phys. 121 (2017) 034302.
[53] A. Delin, P. Ravindran, O. Eriksson, J. Wills, Int. J. Quantum Chem. 69 (1998) 349.
[54] S.Z. Karazhanov, P. Ravindran, A. Kjekshus, H. Fjellvag, B.G. Svensson, Phys. Rev. B 75 (2007) 155104.
[55] P. Ravindran, A. Delin, B. Johansson, O. Eriksson, J.M. Wills, Phys. Rev. B 59 (1999) 1776.
[56] T.V. Vu, H.D. Tong, D.P. Tran, N.T.T. Binh, C.V. Nguyen, H.V. Phuc, H.M. Do, N.N. Hieu, RSC Adv. 9 (2019) 41058.